Soils and Rocks
www.soilsandrocks.com
An International Journal of Geotechnical and Geoenvironmental Engineering
ISSN 1980-9743
ISSN-e 2675-5475

The cavity's effect on the bearing capacity of a shallow footing in reinforced slope sand

Bendaas Azeddine[1#], Merdas Abdelghani[1]

Article

Keywords
Reinforced
Bearing capacity
Sand slope
PVC pipe

Abstract

This paper presents an experimental and numerical study for the effect of the cavity on the behaviour of a strip footing positioned on a reinforced sand slope. This study used a new type of geosynthetics called fiber carbon and fiber glass. These components have the potential to isolate the soil inside the geosynthetic and prevent shears stress mobilization. The investigation aimed to determine the effect of cavity depth (h) and the number of reinforcing layers (N) on the bearing capacity and settlement characteristics of footing, empirically for investigating the effect of cavity on the bearing capacity, some parameters were assumed constant in all tests, for example, relative density, a distance of the footing from the slope edge, and length between layers of reinforcement. The variable parameters are the distance between footings and centre of cavity and the number of reinforcing layers. The results show that the settlement behaviour of footing adjacent to a soil slope is significantly affected by h and N. It is observed that qu, which represents the ultimate bearing capacity, improves with an increase in N. The influence of the cavity appeared insignificant when it was positioned at a depth equal to twice the width of footing.

1. Introduction

Bearing capacity and settlement are important factors in the construction of many types of geotechnical structures, particularly in hilly areas where it is necessary that foundations of those structures to be constructed on sloping grounds. Examples of such projects include buildings, electrical transmission towers, and bridges.

When a footing is constructed near a slope, the bearing capacity is relatively reduced compared to the footing on level ground. Having a strong grasp of the response of footing built close to slopes, particularly slope with a cavity, is crucial to the stability of structures, which can be expressed in terms of factor of safety.

Cavities are associated with tunnels, rail ways and canals, water, sewage, gas pipes, and power lines. All these cavities are affecting the ground stability. Knowing the location of the cavity and the characteristics of the materials formed in the cavities is an essential factor in ensuring the soils stability and choosing good reinforcement (Culshaw & Waltham, 1987).

Under such conditions, solutions such as improving the geometry of sloping surfaces, injections, or use of soil reinforcement are required to improve the bearing capacity of foundations and reinforce the slope with geosynthetic layers (Afshar & Ghazavi, 2014). Soil reinforcement is considered a suitable method for improving the bearing capacity of footing that can widen the road and repair collapsed slopes (Al-Jazaairry & Toma-Sabbagh, 2017; Leshchinsky, 1997).

The literature has shown that the performance of the surface footing can be influenced by other parameters such as the geometrical slope parameters (footing shape, slope angle and height, void size, and void shape), slope soil properties (total unit weight, cohesiveness, and angle of shearing resistance), the type of geosynthetic reinforcement used and the arrangement of the geosynthetic reinforcement layers, depth of top layer, the number and vertical spacing of layers. According to the majority of researchers, placing geosynthetic reinforcing layers at the proper places inside slopes may substantially enhance the bearing capacity and reduce settlements of footings located on the crest of hills. Dahoua et al. (2018) proposed a mathematical approach for estimating the stability of geotextile reinforcements. According to the void size and position, the experimental observation of Kiyosumi et al. (2011) demonstrated three sorts of failure modes for a single void. Upper-bound calculations were presented to interpret the observed changes in bearing capacity.

Kolay et al. (2013) studied a footing placed on double-layer soil to find the load-settlement for reinforced and

[#] Corresponding author. E-mail address: azeddine.bn@yahoo.com
[1] University of Sétif 1, Faculty of Technology, Department of Civil Engineering, Sétif, Algeria.

Submitted on April 10, 2022; Final Acceptance on November 4, 2022; Discussion open until May 31, 2023.
https://doi.org/10.28927/SR.2023.003622

unreinforced soils and noticed that the increment of load-bearing capacity is dependent on the number of reinforcement layers. Zahri et al. (2016) proposed a multi-step method for analysing slope stability in open pit mines.

An investigation of the influence of a cavity on geogrid reinforced soil was carried out by Kapoor et al. (2019). The presence of cavities at specific depths was investigated and an analysis was performed to determine the load-bearing capacity and settlement of a footing on a geogrid-reinforced surface. The Plaxis-2D (v8) finite element package with the Mohr-Coulomb model was used to assess the elastic failure and determine the effect of many factors, such as the number of geogrid layers utilized, the spacing between each successive layer, the position of the cavity and its size, as well as the depth of the footing.

Results of recent research conducted by Zhou et al. (2018) demonstrate that the undrained bearing capacity with voids responds to soil features, and that the failure mechanism is related to numerous soil parameters, the location of single voids, and the straight distance between two voids.

According to Zhao et al. (2018), the stability analysis of asymmetrical cavities is conducted using the upper limit technique. The findings suggest that the local shear failure type is the eldest in the soil around the cavity. The stability is augmented with an increase in the friction angle and reduced with an increase in the horizontal distance and descriptor diameter values.

Xiao et al. (2018) used finite element limit analysis to examine the undrained bearing capacity of strip footing over voids in two-layered clays, and to provide charts and formulas to calculate the undrained bearing capacity factor Ns. The cited authors also examined what effect the various soil properties, including the undrained shear stress ratio, top layer thickness, void size, and spacing of voids have on the Ns factor.

On the other hand, Mansouri et al. (2021) investigated the bearing capacity-settlement of footing on a slope with void and the effect of several factors, such as top vertical distance of void from the base of footing, horizontal space connecting the void-footing center, and load eccentricity where the subterranean void, as well as the critical depth between the soil and the top layer of the void, were found to have an impact on the stability of strip footing.

Baah-Frempong & Shukla (2020) presented the findings of laboratory model testing and numerical analysis for strip footing stability buried in a geotextile-reinforced sand slope and study. The influence of footing embedding depth (D), number of geotextile layers N on bearing capacity and settling properties of the embedded footing was investigated. Results indicate that D and N substantially influence the load-settlement behavior of the embedded footing. It is observed that bearing capacity ratio (BCRu) improves with an increase in N and reduces when D and B increase being D = B (B is the base width), while the highest BCRu was obtained when D/B = 0.

Satvati et al. (2020) developed a novel type of three-dimensional geosynthetic that outperformed geogrid in terms of decreasing soil permeability. They used a laboratory modelling method to examine the effects of different factors on the bearing capacity of footings on soil slopes. The results showed that cylindrical reinforcement has a more significant effect than planar reinforcement in terms of increasing bearing capacity and decreasing settlement under the same circumstances as certain parameters.

Saadi et al. (2020) conducted an experimental investigation on the effect of interference on the bearing capacity of two adjacent foundations in cavitated soil. The results revealed that cavities and dual footing interference affecting the bearing capacity as well as the efficiency factor when the cavity effect is eliminated by increasing the distance between the footing and the cavity. In this study, the cavity's effect on the behavior of geosynthetic reinforced footing on soil slope was investigated to evaluate some important parameters of reinforced soil, because of the lack in the literature of similar studies in this field, a set of laboratory tests to assess the effects mentioned main parameters on the reinforced slopes were performed. The conclusions of this study can be applied to future designs by geotechnical engineers to achieve a better estimation of the bearing capacity of footing on soil slopes. Also, a new type of geosynthetics was used in this study such as carbon and glass fiber reinforced polymer to reinforce the soil slope, so the effects of using this type of geosynthetics to determine the bearing capacity of the shallow footings were evaluated.

2. Experimental study

2.1 Materials

2.1.1 Soil properties

The soil used in this study is sand. Laboratory tests were performed according to test methods described in ASTM Standards to determine the geotechnical properties next; grain distribution tests were performed according to ASTM D422-63 (ASTM, 2007), the values detected of D_{10}, D_{30}, D_{60}, was performed according to ASTM D854-14 (ASTM, 2014), the mean value of specific gravity $G_s = 2.65$ was determined by pycnometer test. According to ASTM D4253-00 (ASTM, 2000), the maximum and the minimum unit weight of the sand was measured and the corresponding values of the minimum and the maximum void ratio were calculated, the relative density of sand bed as $D_r = 60\%$ resulting in a unit weight of 15.75 kN/m^3, direct shear tests were performed according to ASTM D3080-90 (ASTM, 1990) to determine the shear strength parameters (c and φ). Table 1 groups the characteristics of sand and their average values. The particle-size distribution of soil is shown in Figure 1. According to the unified soil classification system (USCS), the soil is classified as poorly graded sand (SP).

Table 1. Properties of sandy soil.

Parameters	value
Specific gravity	2.65
Maximum dry unit weight, $\gamma_{d\,max}$ (kN/m^3)	16.3
Minimum dry unit weight, $\gamma_{d\,min}$ (kN/m^3)	15
Maximum void ratio	0.67
Minimum void ratio	0.50
Relative density, D_r (%)	60
Peak friction angle, φ (°)	38
Cohesion, c (kPa)	1
Uniformity coefficient, C_u	1.83
Coefficient of curvature, C_c	1.08
Effective particle size, D_{10} (mm)	0.185
D_{30} (mm)	0.26
D_{60} (mm)	0.34

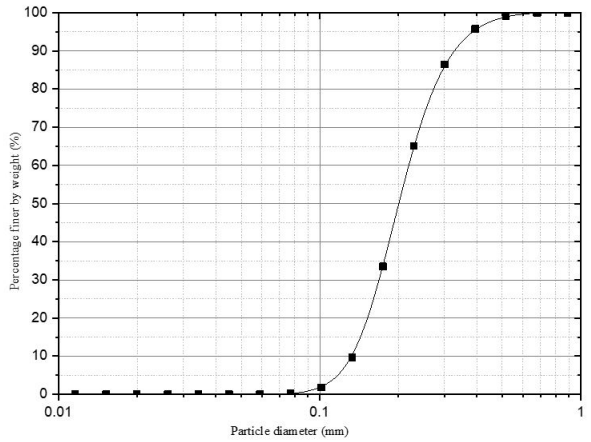

Figure 1. Particle-size distribution of soil.

2.1.2 Geosynthetic properties

Modern geosynthetics such as fiber glass and carbon fiber were used to verify the results of this analysis as seen in Figure 2. The test results for measuring the reinforcing layer tensile strength are presented in Table 2.

2.1.3 Cavity properties

In order to actually simulate a cavity, we are using PVC, the thickness of PVC is 2 mm, and the exterior diameter is 110 mm, in the design of the test model. The parameters of the PVC tube are shown in Table 3.

2.2 Test tank and model footing

The experiment conducted in a test tank with dimensions of 1000 mm × 490 mm in plan and 600 mm in height, two sides of the tank were constructed with rigid steel plates to prevent lateral movement and offer plain strain condition within the soil mass during the test, the back face of the tank was made with a 10 mm-thick transparent glass for

Table 2. Summary of geosynthetics parameters.

Parameters	Fiber glass	Fiber carbon
Color	White	Black
Form	Sheet	Sheet
Thickness (mm)	0.16	0.20
Tensile modulus of elasticity (GPa)	72	231
Elongation (%)	4.9	1.9

Table 3. Properties of the PVC used.

Parameters	Value
Unit weight (kN/m^3)	13.5 - 14.5
Tensile strength (MPa)	45
Elongation %	80
Elastic modulus (MPa)	3000

Figure 2. Fiber glass and carbon fiber elements used in this study.

monitoring the slope failure mechanism or cavity collapse during the test. A steel strip footing of 100 mm × 480 mm in plan and a thickness of 10 mm used for the study. The base length was thus almost equivalent to the tank width for the simple strain state to be retained throughout the test.

2.3 Loading method

We used MTS universal testing system that combines high-performance loading frame technology, ease of use of MTS test suite (TW) software compatible precision sensors, and practical and ergonomic manual terminals. This system includes a load cell capable of applying up to 50 kN on the footing. We apply load at the centroid of the footing to avoid the loading eccentricity effect. The loading speed of this unit can be adjusted to a maximum of 1 mm/min. Since lower-speed loading more accurately simulate static loading conditions, all laboratory experiments are conducted at a speed of 1 mm/min (Figure 3).

2.4 Model preparation method

The sand slope form, sand layers, reinforcement levels and cavity depths are initially marked inside the glass installed

in the tank and the method described in Yoo (2001), Lee & Manjunath (2000), and Sawwaf (2007) is followed for the slope preparation where sand was poured into the tank into 50 mm thick sand layers and manually compacted till achieving the target relative density Dr = 60%. After reaching the cavity height marked h = 150 mm, a circular PVC with a diameter of 110 mm was positioned at the desired height, as shown in Figure 4b. Subsequently, the sand compaction continued until reaching the position of the reinforcement layers in this case. Two types of reinforcement (glass and carbon fiber) were used, with reinforcement layers all along placed at their desired levels (Figure 4a), where the compaction of sand layers is performed after placing each layer of reinforcement as presented in Figure 5. The figure shows, that B represents the footing width, a is the distance of the first layer of reinforcement and the base of the footing (u). The space between two layers of reinforcement, h, illustrates the vertical distance between the cavity and footing, N is the number of reinforcement layers, b is the footing distance from the edge of the slope, and D is the diameter of the cavity. After the slope was established, the surface of the slope was leveled well so that the footing could be placed on a level surface for the stress distribution under the footing and avoid eccentric loading, as shown in Figure 5c. It should be mentioned that the dimensions selected in this analysis of the soil slope are consistent with those used in previous laboratory study (Ueno et al., 1998). Table 4 lists the experiments conducted in this analysis by holding a range of parameters constant and examining other variable parameters effect on load capacity and settlement.

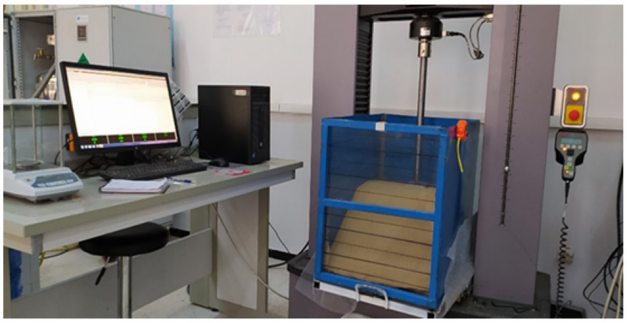

Figure 3. A view of the laboratory model footing load test set-up.

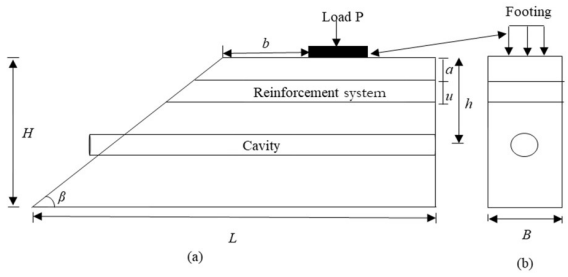

Figure 4. Schematic diagram of a shallow footing near slope: (a) side view and (b) cross-section along the footing.

3. Numerical study

A series of three-dimensional finite-element analyses (FEA) was performed using the software Plaxis 3D to simulate the experimental program. A plane strain model was used to carry out the FEA. The geometry and characteristics of the model used in the finite element analysis are the same as those employed in the laboratory test. A prescribed footing load was used to simulate the rigid footing settlement. The behaviour of sand was simulated using the non-linear Mohr-Coulomb criterion available in Plaxis 3D. The Mohr-Coulomb model has five input parameters: Young's modulus (E), Poisson ratio (ν), friction angle (φ), cohesion (c), and angle of dilatancy (ψ). The modulus of subgrade reaction of the sand bed (ks) can be estimated from the load–settlement curve using the following equation.

$$k_s = \frac{q_{1.25}}{1.25\times10^{-3}}\left[\frac{kN}{m^3}\right] \quad (1)$$

Where q1.25 is the uniform pressure applied to the footing at 1.25 mm of settlement. Was used to find the E values obtained from Equation 2 (Selvadurai, 2013; Shukla & Chandra, 1996). The value of E is dependent on the sand relative density, number of reinforcement layers, and cavity location. Therefore, a unique value of E was utilised in each case studied in the

Table 4. Tests performed in this study.

Series	Constant	Variable
1-fiber glass	βslope = 35° b/B = 1 h/B = 1.5	N = 1; 2; 3
2-fiber carbon	S/B = 0.25 u/B = 0.25 Dr = 60%	N = 1; 2; 3

Figure 5. (a) A carbon fiber layer being installed within the slope; (b) rear view; (c) top view.

numerical simulation. Some Plaxis 3D simulations were conducted and compared to their experimental counterparts to determine an appropriate value for the thickness of the sand bed (H). It was confirmed that a reasonable value of E could be obtained when H was approximately three times the footing width (B) (Kazi et al., 2015; Lovisa et al., 2010). The soil Poisson's ratio (ν) was assumed to be 0.25 for all cases. The angle of dilatancy (ψ) was obtained from the friction angle (φ) using the Equation 3 (Bolton, 1986).

$$E = k_s H\left(1+\nu\right)\left(1-2\nu\right) \quad (2)$$

$$\psi = \varphi - 30° \quad (3)$$

The interaction between the reinforcement layers and the surrounding soil was simulated by interface elements located between the reinforcement layers, and soil. The interface elements are the strength reduction factor Rinter, which was assumed to be 2/3 (Kazi et al., 2015). The foundation was modeled as a plate with a high flexural rigidity (EI) and normal stiffness (EA). The reinforcement fibers were drawn using software (AutoCAD) and then imported to the model as modified geogrid elements as available in the software Plaxis 3D. This option allows the users to define the only required parameter, the elastic normal stiffness (EA), which was determined from the laboratory test conducted on a specimen of the reinforcement layer. The cavity is represented in the study as a circle with a diameter of D = 1B and a wall thickness of 1 mm, to exactly simulate the experimental model. The cavity model system is considered a plane strain condition with 15-node elements. Mohr-Coulomb plasticity model was specified to solid element which symbolizes soil around the PVC pipe. Fifteen nodded plane strain triangular elements were used to model the backfill (Rajkumar & Ilamparuthi, 2008), with a restricted horizontal displacement and free vertical displacement. The other parameters used for the numerical analysis are well defined in the Plaxis 3D guide. The numerically simulated model is as shown in Figure 6.

The initial stress within the slope was determined by gravity loading, this method was utilized because the slope is not a horizontal surface. In Plaxis 3D the load–settlement analysis of a footing can be done, by either the prescribed footing load method (load controlled) or prescribed displacement method (displacement controlled). A prescribed displacement was applied to the footing in increments accompanied by iterative analysis until the failure occurred.

The study consists of two stages, the first one deals a prescribed displacement applied to the footing with increments until the failure occurred without reinforcement. To reduce the effect of surface load on the cavity and improve its performance, the fiber reinforcements were used in the second stage. Table 5 summarizes the material properties used in the analysis.

4. Results and discussion

4.1 Experimental results

Findings from the results of small-scale laboratory model tests performed to evaluate the ultimate bearing capacity of a footing with a width B = 100 mm placed at a constant edge distance ratio b/B = 1 on sand slope with a variable cavity depth ratio h/b = 0.5B, 1B, 1.5B in a single (N =1) double (N = 2) and triple (N = 3) layers of carbon and glass fiber reinforcement for a sand slope having an angle of inclination β = 35° to the horizontal and a relative density Dr = 60%. In all the experiments carried out, the reinforcing layers were stretched from the slope face to the rear of the test tank. The first (top) layer was installed at a constant depth ratio of u/B = 0, 25 below the footing base. A consistent vertical spacing ratio s/B = 0.25 was maintained between the subsequent layers and the initial layer during installation.

The load-settlement curves of the footing can be used to determine the ultimate bearing capacity of the footing. The highest possible value of q is defined through the peak in the applied pressure-settlement curve. It is possible to accurately define the peak value of q (of peak) by referring to the applied pressure-settlement curve, based on the procedure suggested by Vesić (1973) and Terzaghi et al. (1996). According to this approach, qu is the point on the load-settlement curve at which the curve becomes steep and straight.

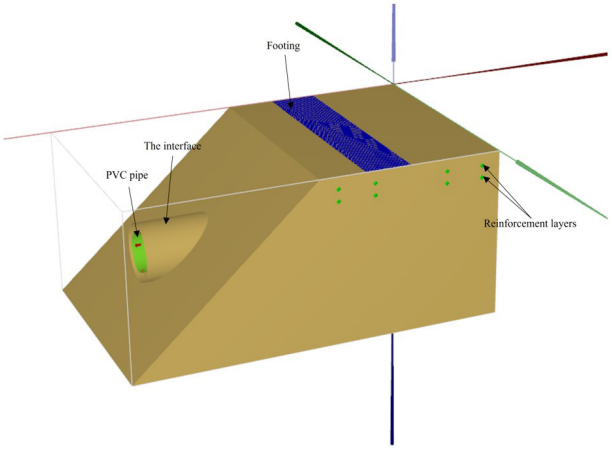

Figure 6. Plot of geometry model with boundary conditions.

Table 5. Parameters used in the numerical analysis.

Parameter for soil	Parameter of fiber	Parameter of footing
E = 3000-4500 (kN/m^3)	Glass fiber	EA = 640000 (kN/m)
φ = 38 °	EA = 400 (kN/m)	EI = 85 (kN/m^2)
ψ = 8°	Carbon fiber	Thickness = 0.01 m
γ_d = 15.75 kN/m^3	EA = 600 (kN/m)	
ν = 0.25		
c = 1 kPa		
Rinter= 2/3		

The laboratory test results are presented as load (q)-settlement (s) curves where s is the settlement of the footing corresponding to a particular q and B the footing width. It is observed that as the footing's applied pressure q increases, the settlement (s) also increases until the footing fails. It is also observed that in the case of unreinforced soil, the effect of the cavity on the bearing capacity of the footing is estimated based on the optimum cavity depth in different values of 3B, 2.5B, 2B, and 1.5B. The ultimate bearing capacity values obtained are 4.55 kN, 3.38 kN, 2.86 kN, and 2.37 kN respectively, with Figure 7 illustrating the maximum effect of the cavity on the bearing capacity of the footing in depth 1.5B. As a result, 1.5B is used to calculate the cavity effect in different reinforcement layer numbers, N = 1, N = 2, N = 3.

Figure 8 shows the influence of number of reinforcement layers N of glass fiber for a cavity depth h/B =1.5. The figure shows that increasing the number of reinforcement layers improves the load-bearing capacity q from 13% to 88%, and 88% to 258%, for N = 0 (unreinforced), N = 1, N = 2, and N = 3, respectively.

In Figure 9 is observed that qu increases with N. The footing bearing capacity significantly improves from 46% to 143%, and 143% to 424% for reinforced with carbon fiber single layer, double layer, triple-layer respectively.

Figure 10 shows a comparison between the different types of reinforcements used in this study. It is observed that carbon fibers have a greater improvement to the load bearing capacity of the footing in comparison with glass fiber, this difference is significantly apparent when using multiple reinforcement layers.

4.2 Numerical results and comparison

In finite element modeling, a finer mesh typically results in a more accurate solution. However, as mesh is made finer, the computation time increases. Mesh convergence study is thus performed to obtain a satisfactory tradeoff between the accuracy and computing resources. Figure 11 shows mesh convergence analysis carried out on model unreinforced slope. It can be observed that as mesh gets finer, the results converge. But there is no significant difference between the medium and the fine mesh. The medium mesh was selected for the present study because it takes a shorter duration to complete the modelling than the fine and very fine meshes. Figure 12 show the deformed mesh for a typical analysis. Displacements and stress concentration in a typical model are presented in Figures 13-14.

Figures 15-16 show a comparison of the load settlement curves of the experimental and the FEA results for all specimens. These results indicate that the FEA model was able to accurately predict the behavior of the reinforced soil. Furthermore, the use of both carbon and glass fibers resulted in a significant increase in the load-bearing capacity of the footing. It is clearly noticed that the numerical values closely follow the experimental values. Some variations are well expected because of the in-built limitations of the Plaxis to simulate the behaviour of unreinforced and reinforced soils.

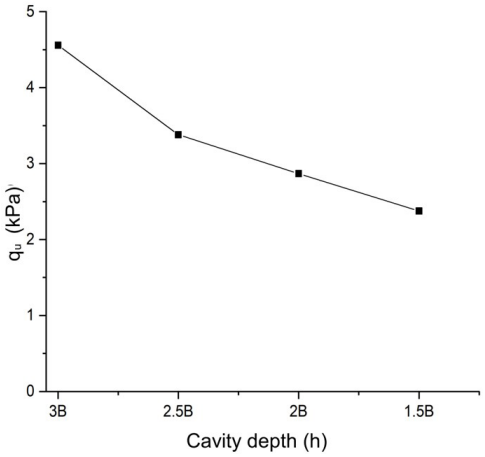

Figure 7. Variation of ultimate bearing capacity qu with cavity depth ratio.

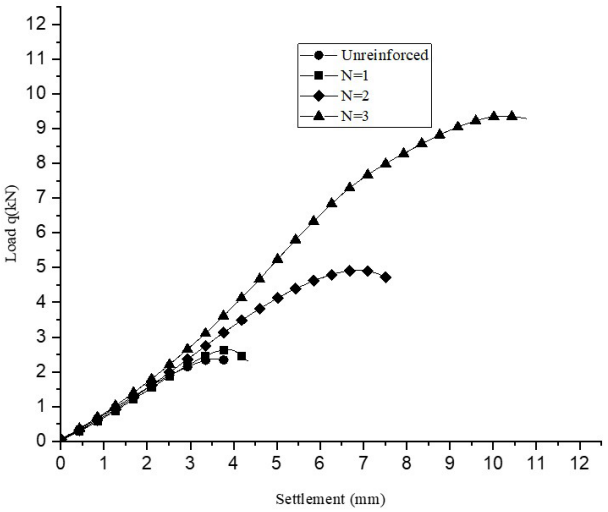

Figure 8. Effect the number of reinforcing layers N for glass fiber on load-bearing pressure (q) and settlement.

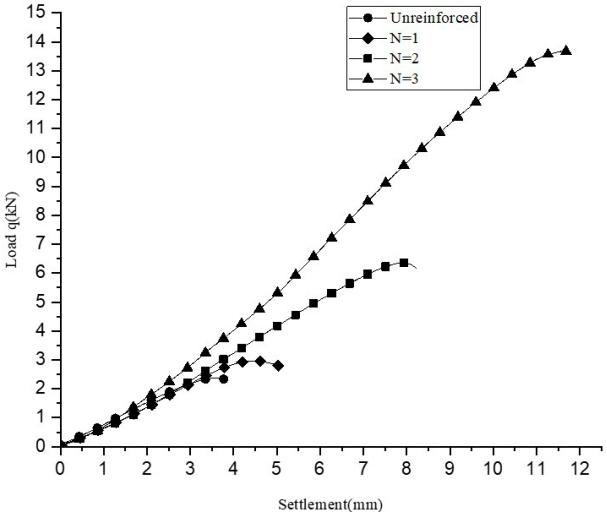

Figure 9. Effect the number of reinforcing layers N for carbon fiber on load-bearing pressure (q) and settlement.

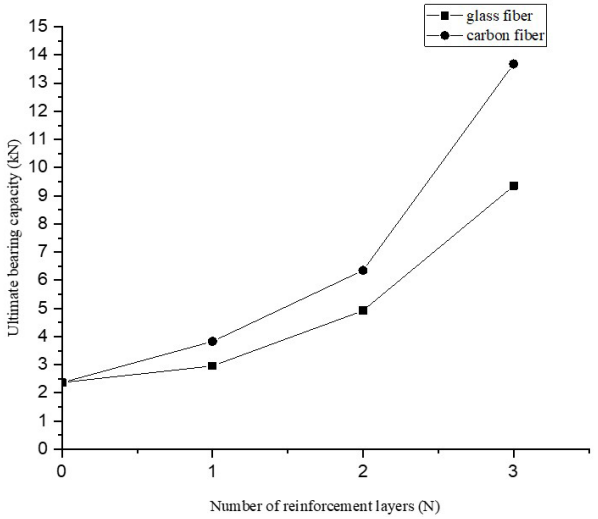

Figure 10. Comparison of ultimate bearing capacity with number of reinforcement layers N from carbon and glass fiber.

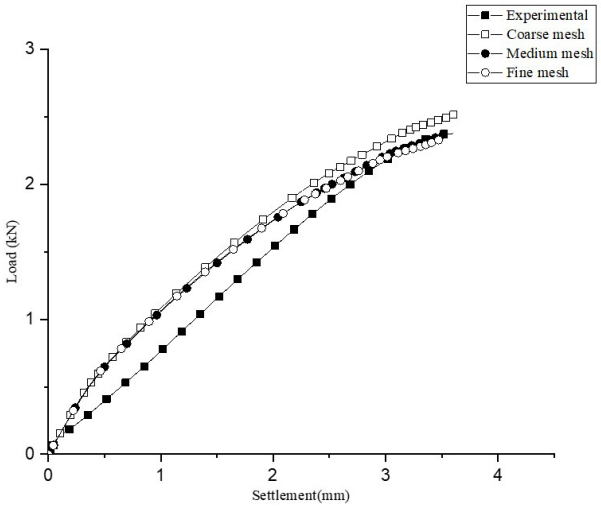

Figure 11. Mesh convergence study.

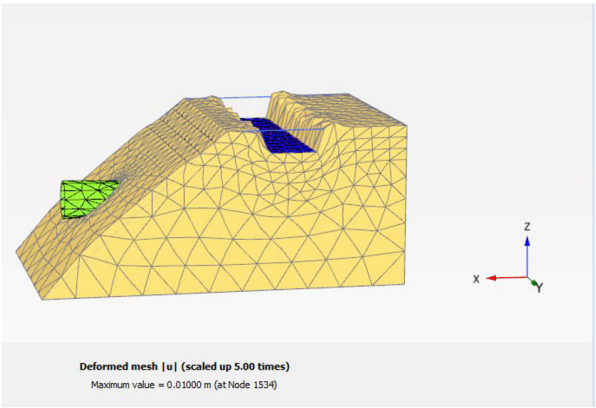

Figure 12. Deformation of mesh of a typical finite-element model with reinforcement.

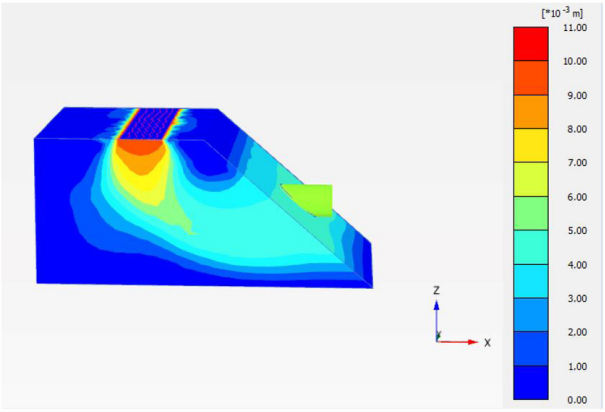

Figure 13. Typical displacement shading contours (in meters).

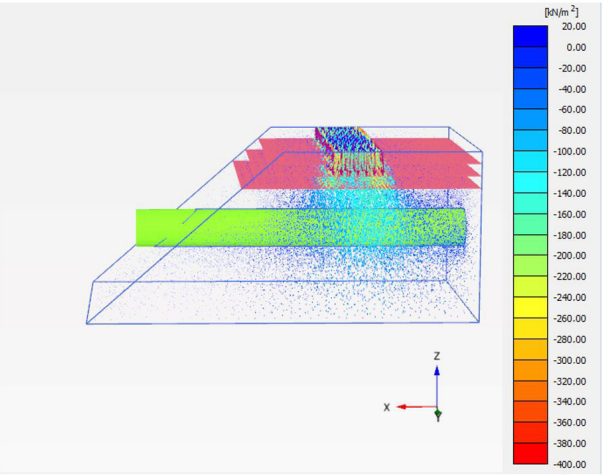

Figure 14. Stress concentration (in kPa).

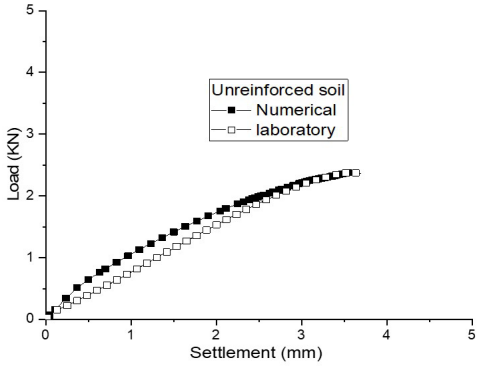

Figure 15. Comparison of load-settlement curves in unreinforced soil case.

Figure 17 compares the ultimate bearing capacities obtained from the numerical simulations to those established from the laboratory model tests for different reinforcement types used in this study. It is observed that the ultimate bearing capacities are in good agreement.

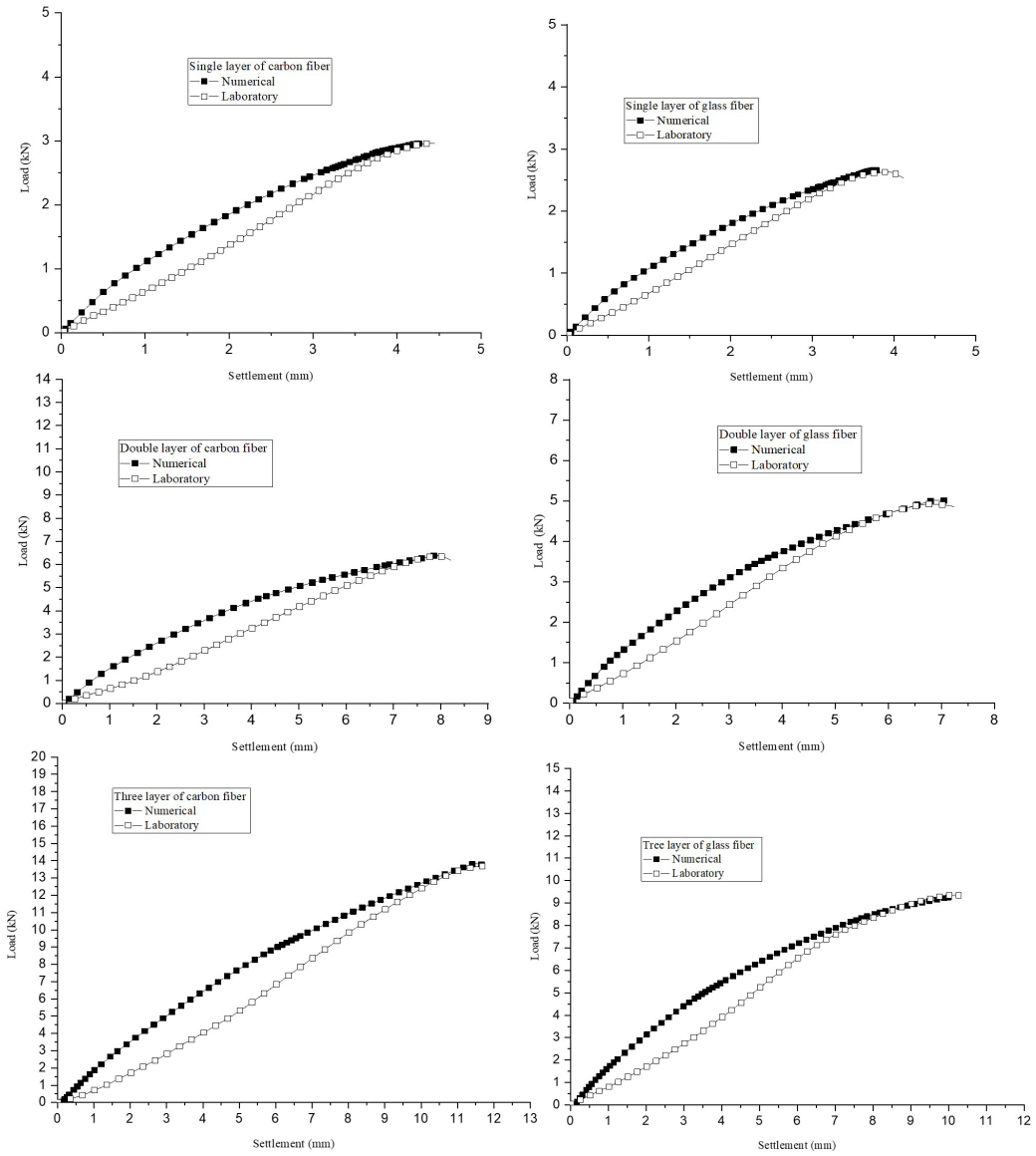

Figure 16. Comparison of load-settlement curves in reinforced soil cases.

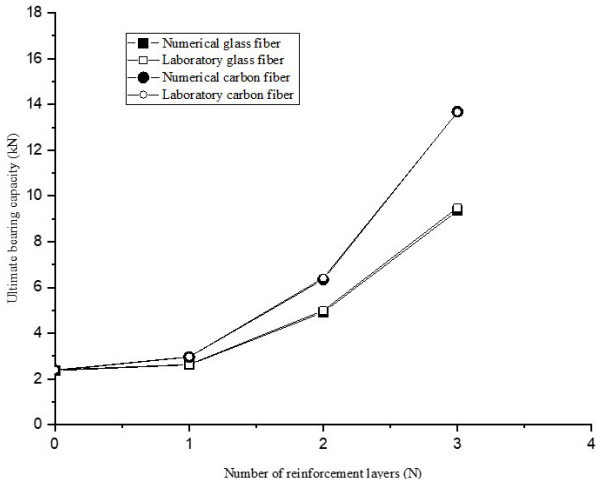

Figure 17. Comparison of the ultimate bearing capacity qu from experimental and numerical studies.

5. Conclusions

For the purpose of evaluating the effect of the cavity on the bearing capacity and settlement of a footing in sand slope reinforced with a multilayer carbon and glass fibers, a series of laboratory model experiments were carried out. In this study, specifically, to show the relationship between the cavity depth ratio h/B, the number of reinforcing layers N and type of reinforcement on the bearing capacity and settlement characteristics of the footing. The following are the most important conclusions that can be drawn from the findings:

- The cavity depth D, below the slope crest, significantly affects the bearing capacity and settlement characteristics of the footing, the risk of collapse increases when the distance between the cavity and the base is small. Where the bearing capacity of the footing is

directly proportional to the cavity depth. The greater the depth from 1.5b to 2b, 2b to 2.5b, and 2.5b to 3b the greater the bearing capacity from 20% to 42% and from 42% to 91%.

- Using glass and carbon fibers as a reinforcement significantly increases the load bearing capacity of the footing.
- The footing ultimate bearing capacity (q_u) increases with the increase in the number of reinforcing layers (N), by 46%, 143% and 424% for N = 1, N = 2 and N = 3, respectively.
- The use of carbon fibers in reinforcement resulted in significantly higher bearing capacity by up to 46% compared to the glass fibers.
- The results obtained from the finite element analysis using the software Plaxis follow the experimental results closely, at the lower settlement values in all cases, but for higher relative density cases, the results are almost identical.
- The numerical results of the ultimate bearing capacity (qu) of the footing are identical with their experimental counterpart.

Declaration of interest

The authors have no conflicts of interest to disclose.

Authors' contributions

Bendaas Azeddine: methodology, investigation, data curation, writing. Merdas Abdelghani: supervision, validation.

Data availability

The datasets generated and analyzed in the course of the current study are available from the corresponding author upon reasonable request.

List of symbols

a	depth of reinforcement from base of footing
b	edge distance of footing from slope crest
c	cohesion
C_c	coefficient of curvature
C_u	uniformity coefficient
h	embedded depth of cavity
qu	ultimate bearing capacity of footing
u	vertical spacing between reinforcement layers
B	width of footing
D_r	relative density of sand
D_{10}	particle diameter corresponding to 10% finer by weight
D_{30}	particle diameter corresponding to 30% finer by weight
D_{60}	particle diameter corresponding to 60% finer by weight
E	Young's modulus
EA	normal stiffness
EI	flexural rigidity
H	slope height
Ks	modulus of subgrade reaction
N	number of reinforcement layers
Rinter	strength reduction factor
β	slope angle
$\gamma_{d\,max}$	maximum dry unit weight
$\gamma_{d\,min}$	minimum dry unit weight
γ_d	dry unit weight
φ	angle of internal friction
ν	Poisson's ratio
ψ	angle of dilatancy

References

Afshar, J.N., & Ghazavi, M. (2014). A simple analytical method for calculation of bearing capacity of stone-column. International Journal of Civil Engineering, 12(1), 15-25.

Al-Jazaairry, A.A., & Toma-Sabbagh, T.M. (2017). Effect of cavities on the behaviour of strip footing subjected to inclined load. International Journal of Civil, Environmental, Structural, Construction and Architectural Engineering, 11(3), 292-298.

ASTM D3080-90. (1990). Standard Test Method for Direct Shear Test of Soils Under Consolidated Drained Conditions. ASTM International, West Conshohocken, PA.

ASTM D422-62. (2007). Standard Test Method for Particle-Size Analysis of Soils. ASTM International, West Conshohocken, PA. https://doi.org/10.1520/D0422-63R07E02.

ASTM D4253-00. (2000). Standard Test Methods for Maximum Index Density and Unit Weight of Soils Using a Vibratory Table. ASTM International, West Conshohocken, PA.

ASTM D854-14. (2014). Standard Test Methods for Specific Gravity of Soil Solids by Water Pycnometer. ASTM International, West Conshohocken, PA. https://doi.org/10.1520/D0854-14.

Baah-Frempong, E., & Shukla, S.K. (2020). Behaviour of a strip footing embedded in a sand slope reinforced with multilayer geotextile. Indian Geotechnical Journal, 50(4), 560-576. http://dx.doi.org/10.1007/s40098-019-00393-3.

Bolton, M.D. (1986). The strength and dilatancy of sands. Geotechnique, 36(1), 65-78. http://dx.doi.org/10.1680/geot.1986.36.1.65.

Culshaw, M.G., & Waltham, A.C. (1987). Natural and artificial cavities as ground engineering hazards. Quarterly Journal of Engineering Geology and Hydrogeology, 20(2), 139-150. http://dx.doi.org/10.1144/GSL.QJEG.1987.020.02.04.

Dahoua, L., Usychenko, O., Savenko, V.Y., & Hadji, R. (2018). Mathematical approach for estimating the stability of geotextile-reinforced embankments during an

earthquake. Mining Science, 25, 207-217. http://dx.doi.org/10.5277/msc182501.

Kapoor, A., Walia, B.S., & Singh, C. (November 2-3, 2019). Effect of cavity on bearing capacity of shallow foundation in reinforced soil. In H. Singh, P. Garg, & I. Kaur (Eds.), Proceedings of the 1st International Conference on Sustainable Waste Management through Design (pp. 313-322). Cham, Switzerland: Springer. https://doi.org/10.1007/978-3-030-02707-0_37.

Kazi, M., Shukla, S.K., & Habibi, D. (2015). An improved method to increase the load-bearing capacity of strip footing resting on geotextile-reinforced sand bed. Indian Geotechnical Journal, 45(1), 98-109. http://dx.doi.org/10.1007/s40098-014-0111-9.

Kiyosumi, M., Kusakabe, O., & Ohuchi, M. (2011). Model tests and analyses of bearing capacity of strip footing on stiff ground with voids. Journal of Geotechnical and Geoenvironmental Engineering, 137(4), 363-375. http://dx.doi.org/10.1061/(ASCE)GT.1943-5606.0000440.

Kolay, P., Kumar, S.K.P., & Tiwari, D. (2013). Improvement of bearing capacity of shallow foundation by using geogrid reinforced double layered soil. Journal of Construction Engineering, 2013, 293809.

Lee, K.M., & Manjunath, V.R. (2000). Experimental and numerical studies of geosynthetic-reinforced sand slopes loaded with a footing. Canadian Geotechnical Journal, 37(4), 828-842. http://dx.doi.org/10.1139/t00-016.

Leshchinsky, D. (1997). Design procedure for geosynthetic reinforced steep slopes. Washington DC: US Army Corps Engineers. Retrieved in November 4, 2022, from https://apps.dtic.mil/sti/citations/ADA321646.

Lovisa, J., Shukla, S., & Sivakugan, N. (2010). Behaviour of prestressed geotextile-reinforced sand bed supporting a loaded circular footing. Geotextiles and Geomembranes, 28(1), 23-32. http://dx.doi.org/10.1016/j.geotexmem.2009.09.002.

Mansouri, T., Boufarh, R., & Saadi, D. (2021). Effects of underground circular void on strip footing laid on the edge of a cohesionless slope under eccentric loads. Soils and Rocks, 44(1), 1-10. http://dx.doi.org/10.28927/SR.2021.055920.

Rajkumar, R., & Ilamparuthi, D.K. (2008). Experimental study on the behaviour of buried flexible plastic pipe. The Electronic Journal of Geotechnical Engineering, 13, 1-10.

Saadi, D., Abbeche, K., & Boufarh, R. (2020). Model experiments to assess effect of cavities on bearing capacity of two interfering superficial foundations resting on granular soil. Studia Geotechnica et Mechanica, 42(3), 222-231. http://dx.doi.org/10.2478/sgem-2019-0046.

Satvati, S., Alimohammadi, H., Rowshanzamir, M., & Hejazi, S.M. (2020). Bearing capacity of shallow footings reinforced with braid and geogrid adjacent to soil slope. International Journal of Geosynthetics and Ground Engineering, 6(4), 1-12. http://dx.doi.org/10.1007/s40891-020-00226-x.

Sawwaf, M.A. (2007). Behavior of strip footing on geogrid-reinforced sand over a soft clay slope. Geotextiles and Geomembranes, 25(1), 50-60. http://dx.doi.org/10.1016/j.geotexmem.2006.06.001.

Selvadurai, A.P.S. (2013). Elastic analysis of soil-foundation interaction. Amsterdam: Elsevier.

Shukla, S.K., & Chandra, S. (1996). A study on a new mechanical model for foundations and its elastic settlement response. International Journal for Numerical and Analytical Methods in Geomechanics, 20(8), 595-604. http://dx.doi.org/10.1002/(SICI)1096-9853(199608)20:8<595:AID-NAG835>3.0.CO;2-9.

Terzaghi, K., Peck, R.B., & Mesri, G. (1996). Soil mechanics in engineering practice. Hoboken: John Wiley & Sons.

Ueno, K., Miura, K., & Maeda, Y. (1998). Prediction of ultimate bearing capacity of surface footings with regard to size effects. Soil and Foundation, 38(3), 165-178. http://dx.doi.org/10.3208/sandf.38.3_165.

Vesić, A.S. (1973). Analysis of ultimate loads of shallow foundations. Journal of the Soil Mechanics and Foundations Division, 99, 45-73. http://dx.doi.org/10.1061/JSFEAQ.0001846.

Xiao, Y., Zhao, M., & Zhao, H. (2018). Undrained stability of strip footing above voids in two-layered clays by finite element limit analysis. Computers and Geotechnics, 97, 124-133. http://dx.doi.org/10.1016/j.compgeo.2018.01.005.

Yoo, C. (2001). Laboratory investigation of bearing capacity behavior of strip footing on geogrid-reinforced sand slope. Geotextiles and Geomembranes, 19(5), 279-298. http://dx.doi.org/10.1016/S0266-1144(01)00009-7.

Zahri, F., Boukelloul, M.L., Hadji, R., & Talhi, K. (2016). Slope stability analysis in open pit mines of Jebel Gustar career, NE Algeria–a multi-steps approach. Mining Science, 23, 137-146.

Zhao, L., Huang, S., Zhang, R., & Zuo, S. (2018). Stability analysis of irregular cavities using upper bound finite element limit analysis method. Computers and Geotechnics, 103, 1-12. http://dx.doi.org/10.1016/j.compgeo.2018.06.018.

Zhou, H., Zheng, G., He, X., Xu, X., Zhang, T., & Yang, X. (2018). Bearing capacity of strip footings on c–φ soils with square voids. Acta Geotechnica, 13(3), 747-755. http://dx.doi.org/10.1007/s11440-018-0630-0.